# An Agent-Based Microscopic Pedestrian Flow Simulation Model for Pedestrian Traffic Problems

Shaobo Liu, Siuming Lo, Jian Ma, and Weili Wang

*Abstract*—Guaranteeing a safe, efficient, and comfortable traveling system for pedestrians is one of the most important aspects of an intelligent transportation system. The microscopic simulation of pedestrian flow has attracted increasing research attention in recent years since a reliable simulation model for pedestrian flow may greatly benefit engineers and operators in mass transportation management, as well as designers and planners in urban planning and architecture. This paper introduces CityFlow, an agent-based microscopic pedestrian flow simulation model. The building floor plan in the model is represented by a continuous space constructed in a network approach, and each pedestrian is regarded as a self-adapted agent. Agent movement is implemented in a utility maximization approach by considering various human behaviors. The influences of parameters in the model on the simulation results are investigated. Typical pedestrian flow phenomena, including the unidirectional and bidirectional flow in a corridor as well as the flow through bottlenecks, are simulated. The simulation results are further compared with empirical study results. The comparison reveals that the model can approach the density–speed fundamental diagrams and the empirical flow rates at bottlenecks within acceptable system dimensions. The simulation results of the bidirectional pedestrian flow also show that the model can reproduce the lane-formation phenomenon.

*Index Terms*—Agent-based modeling, fundamental diagram, lane formation, pedestrian flow, utility maximization.

## I. INTRODUCTION

PEDESTRIAN dynamics is related to various transportation system problems. On the one hand, pedestrians are the most vulnerable element of a mass transportation system. Therefore, understanding pedestrian walking behavior and the interaction of pedestrians with the environment is important to ensure pedestrian safety. On the other hand, the high density of crowds in mass transit terminals, such as train stations,

airports, and bus stops, causes serious congestion problems. Knowledge of pedestrian dynamics in these areas can be used to manage crowd movement and to provide insights for urban planners, building designers, and mass transit system operators. Therefore, as a part of an intelligent transportation system, the safety, efficiency, and comfortableness of a pedestrian traveling system would benefit from study of pedestrian dynamics within which pedestrian flow modeling can provide a powerful tool for these purposes.

In fact, empirical study and computer modeling of pedestrian movement under various conditions have been conducted in the past few decades [1]. Field observations [2]–[7] and laboratory experiments [8]–[12] were conducted to understand collective pedestrian flow behavior. These observations and experiments encouraged research on the data collection technology and methodology of pedestrian movement [12], [13]. A large volume of empirical studies focused on several of the most basic indicators of pedestrian flow features, including the so-called fundamental diagrams that show the relationship between pedestrian density and movement velocity or flow rate [2], [4], [8], [12], [14], the flow rate through bottlenecks with different dimensions [3], [5], [9]–[11], and the free walking speed in various conditions [6].

Numerous computer simulation models have been developed so far. Except for some attempts on modeling pedestrian dynamics on a macroscopic level [15], [16], most of existing microscopic pedestrian flow simulation models can be categorized into grid-based discrete models and continuous models based on their representation method of space and time [1], [17], [18]. A representative grid-based discrete model is the Cellular Automata model [19], in which the 2-D floor plan is divided into uniformly distributed grids and pedestrians are allowed to move from one grid to another at each time step depending on the conditions of adjacent grids. Force-based models are one of the most popular modeling paradigms of continuous models [18], [20]. In force-based models, Newtonian mechanics in a continuous space are used to interpret pedestrian movement as the physical interaction between the people and the environment. Both types of models have been used to simulate basic pedestrian flow phenomena, such as the unidirectional or bidirectional flow in a corridor [21]–[23], the crowd passing through a bottleneck [20], [24], the crossing pedestrian flow at intersections [25], [26], and the emergency evacuation from buildings [27]–[29].

However, grid- or force-based models suffer from limitations caused by their own modeling rules. Grid-based models may cause unrealistic results because of overdiscretization of space and time, such as the dilemma of choosing the grid

and time-step sizes, the disagreement between discretized and real dimensions, the diagonal movement trajectories, and the limited speed range and maximum density [17]. Force-based models are accused of some artifacts introduced by their force representation of human behavior. Some of these artifacts include the superposition of mutually exerted repulsive forces in a long range, which may lead to unrealistic backward movement, and the analogy with Newtonian laws, which may cause overlapping of pedestrian bodies and oscillation of movement trajectories [18].

Another type of frequently mentioned model is the agent-based model for crowd dynamics [24], [28], [30]–[32]. Agent-based models, which are sometimes referred to as models based on multiagent systems (MAS) in a more general way, are advanced in terms of flexibility, extensibility, and capability to realize heterogeneity [33], [34]. Pedestrians in this type of model are usually treated as autonomous individuals with self-adaptation abilities. From this point of view, some of the grid- and force-based models can be also placed into the agent-based paradigm because they can be easily extended to incorporate individual features. For example, the Cellular Automata model can be regarded as a degenerated MAS with fixed dense space discretization and synchronous agent behaviors [35]. However, most existing agent-based models also suffer from the aforementioned limitations. Although these artifacts can be reduced by incorporating extra rules, elaborate calibrations and high computing costs are necessary for this action. Only a limited number of microscopic models have considered simulation paradigms other than grid- or force-based ones. For example, Hoogendoorn [36] proposed a microscopic pedestrian modeling theory by assuming pedestrians as adaptive controllers that minimize the subjective predicted cost of walking. However, the framework posed difficulties on implementing the governing equations and validating the model parameters. Antonini *et al.* [31] developed a discrete choice model by defining the pedestrian's choice set as consisting of a combination of three speed regimes and 11 directions within the visual field. The model shows great flexibility to represent pedestrian movement behaviors in a natural manner. However, the large number of parameters leads the model calibration process to a very detailed analysis of the movement direction choice behavior, and its performance on modeling real pedestrian dynamics at the quantitative level is still not clear. Asano *et al.* [30] employed a two-player game to represent movement speed and direction choice behavior by considering explicit collision avoidance and tactical route choice behavior. Another recently published model by Moussaid *et al.* [37] has used a similar concept of human behavioral heuristics based on visual field representation; however, a force-based unintentional collision avoidance mechanism is employed in this model. Moreover, these two models have focused only on the behavior of minimizing travel time and avoiding collisions. Pedestrian behavior is more complicated in reality. For example, people may perceive the movement directions of surrounding pedestrians and follow the ones heading to the same destination while avoiding conflicts with facing pedestrians. This behavior is a natural way to avoid conflicts and maximize the efficiency of pedestrian flow. It may also account for the formation of pedestrian lanes in the bidirectional flow. However, this factor is missing in these two models.

Given the limitations of existing simulation models, finding a feasible modeling approach based on a modeling paradigm that can overcome these limitations and validating the model using real pedestrian data are still necessary. This paper proposes a novel pedestrian flow simulation model, namely, CityFlow. This model can import the building geometry in the format of "DXF" files (the Drawing Exchange Format developed by Autodesk for enabling data interoperability between AutoCAD and other programs) and represents the floor plan as a continuous space with a network structure. Pedestrians are modeled as autonomous agents who can walk through the building guided by routes generated from the route network within the continuous space. Agent movement at every step is realized by an agent-based microscopic pedestrian flow simulation model. The model differs from traditional modeling methods in three ways. First, it is neither grid- nor force-based but will benefit from representing a pedestrian as an agent with a cognitive view range. Second, a novel utility maximization approach is used to mimic the movement behavior of agents by considering several important factors, including perceiving the movement directions of surrounding pedestrians, which are neglected by most existing models. Third, the empirical results on fundamental speed–density relationships are also incorporated into the model to control the movement speed directly. This paper introduces the overall framework of the model and focuses on introducing and validating the agent-based microscopic pedestrian flow simulation model by performing parameter sensitivity analyses, as well as by comparing the simulation results with published empirical data. The model can serve as a computational tool to provide information to assist decision makers under a variety of circumstances related to pedestrian dynamics. Taking the planning, design, and management of mass transportation terminals as an example, the model would be useful for designing and maintaining a safe and efficient pedestrian traffic system, which is also one of the important targets of an intelligent transportation system.

## II. SIMULATION MODEL: CITYFLOW

CityFlow is a new computer simulation model for pedestrian flow that has been recently developed by City University of Hong Kong. This section gives a brief introduction of the model framework and a detailed description of the agent-based microscopic pedestrian movement simulation model used in CityFlow.

### A. Architecture Overview

Fig. 1 shows an overview of the architecture of the model. First, information on the environment, the properties of the agents to be simulated, and the demand of the pedestrian system are required as inputs for the model. The floor plan in the simulation is represented in a network approach by dividing the geometry into "zones" connected to one another by "connections." Fig. 2 shows an example of the floor plan network representation. Each zone is defined in a 2-D continuous space by lines specifying the geometry boundaries. Zones in the
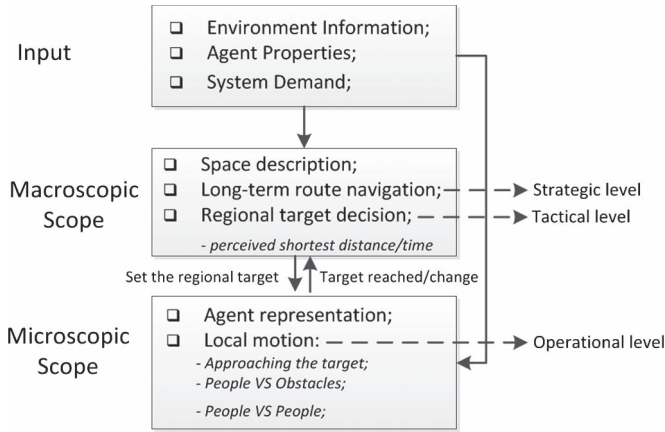
Fig. 1.   Architecture of the simulation model in overview.

building geometry are connected by "arcs," which are actually virtual links between zones representing the features of routes, including distance, type (stair, ramp, walkway, etc.), and capacity of a route (see Fig. 2). In practice, this network structure is generated in the model by reading the preprocessed AutoCAD drawing in DXF format. After this step, the system demand can be set up through an Origin–Destination matrix that defines all the possible routes and their properties, including the flow rate at the source, the construction of every type of pedestrian, and the probabilities of choosing every route.

Similar to most pedestrian flow simulation models, our model is implemented in two levels. Here, we refer to the similar concept proposed by Hoogendoorn and Bovy [38]: the strategic and tactical level behavior in the macroscopic scope and the operational level behavior in the microscopic scope. The macroscopic scope mainly deals with the long-term route choice and map navigation tasks to decide a route and obtain a regional perceivable target. The microscopic scope decides the local movement of the agents at every time step. These scopes are executed by two modules with communications between them: the *route choice and map navigation module* and the *agent-based individual movement module*. The first module identifies the temporary desired regional target of movement. The second module uses this information as the target to govern the actual movement and then calculates the real movement direction and distance in the next time step based on detailed environmental information. Given that this paper focuses on the simulation model for microscopic pedestrian movement, the first module is simply based on the shortest distance rule. Nevertheless, a more sophisticated model will be established in subsequent studies. When the target is reached, the second module will convey this message back to the first module and request for the next target until a connection for this region is reached. The agent will then move to the next region and be assigned the next desired target and so on.

### B. Modeling of Movement Behavior

The agent-based individual movement module is implemented at the microscopic scope. Upon receiving the regional target position from the route choice and map navigation module, the agent is required to move step by step toward the target while adjusting the movement speed according to the

environment and avoiding collisions with other pedestrians and obstacles. An agent in the model is represented by a circle with a view range (see Fig. 3) because a circle will greatly benefit from geometrical calculation in programming. In this paper, the diameter of the circle is set to $r$ ($r = 0.4$ m, which is the typical body size of a person). Theoretically, a pedestrian has infinite choices of walking direction in the view range. In practice, a simplified alternative approach is used to reduce the computational burden without losing accuracy, as suggested by Antonini *et al.* [31]. The view angle $\theta$ is discretized into subangles every $\Delta\theta$. As suggested in [31], we also use $\theta = 170°$, but with uniformly distributed $N$ directions. That is, $\Delta\theta = \theta/N$, where $N$ can be an integer within a reasonable range. The effect of different values of $N$ on the simulation results will be discussed later in this paper. The angle of a possible movement direction $k$ can be denoted by $\theta_k = k \cdot \Delta\theta$, $k \in (0 \sim N)$ (see Fig. 3). The angle of the current movement direction can be denoted by $\theta_c = \Delta\theta \cdot N/2$. The depth of the view range $R$ is set to 3 m in the current model; however, this value can be changed to adapt to different situations, as suggested in [32]. Only the area within the view range is considered effective to make a decision. As shown in Fig. 3(a), assuming that the subject agent $i$ located at $M_{i,t}$ at time $t$ moves at its current velocity $\vec{v}_c$, if the direction $k$ is chosen as its direction in the next time step, the agent will move one step $(\Delta t | \vec{v}_k|)$ based on the new velocity $\vec{v}_k$ on direction $k$ to the position $M_{i,t+1}$ at time $t + 1$. The decision to choose direction $k$ is made by a utility maximization approach, in which a value is assigned as the utility for each $k$, representing the strength of pedestrians' willingness to move in this direction. The utility can be calculated through (1) by considering several factors that may affect the pedestrians' choices. The direction with the strongest utility is selected. Special situations that cause symmetrically distributed utilities should be also considered. For example, considering that people in most regions around the world have a right-hand choice habit, the direction in the right is chosen if the largest value is found for more than one direction. That is

$$U_k = \omega_e \cdot E_k + \omega_o \cdot O_k + \omega_p \cdot P_k + \omega_a \cdot A_k + \omega_i \cdot I_k + \xi \tag{1}$$

where $\omega_e \sim \omega_1$ are the weight parameters used to adjust the sensitivity of each factor and $\xi$ is a stochastic variable used to adjust zero and minus value errors. Other symbols at the right side of the function represent the desire of pedestrians to approach the target as well as the interaction between the pedestrians and the environment and between different pedestrians. These factors are explained in detail in the following discussion.

*1) Efficiency of Approaching the Target Point $E_k$:* This factor can be measured by either the distance from the future position $M_{i,t+1}$ [see Fig. 3(a)] to the target or the angle between the direction $k$ and the direction toward the target. However, for the convenience of limiting the value of $E_k$ within a controllable range, such as [0, 1], we use the following function to calculate for $E_k$:

$$E_k = 1 - \frac{D_{k,t} - (R - R_{k,\text{step}})}{2R_{k,\text{step}}} \tag{2}$$
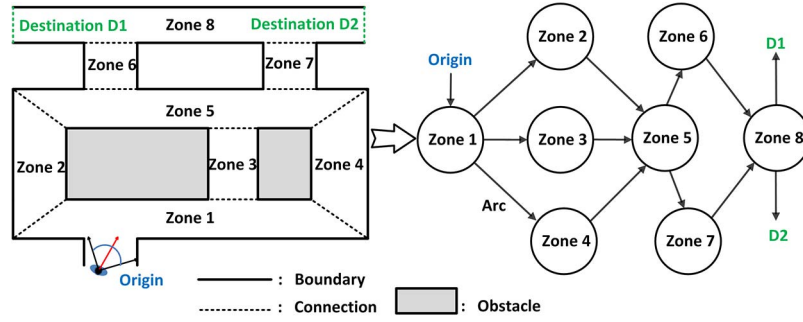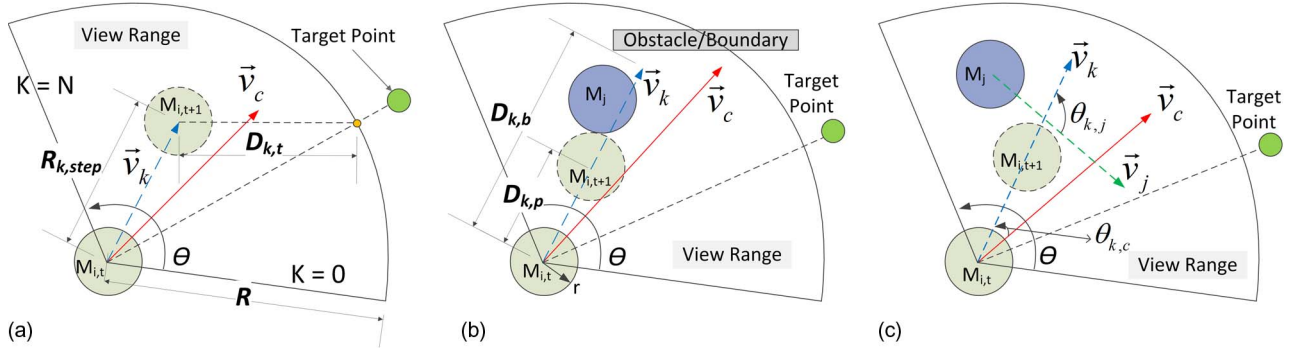
Fig. 2. Illustration of the floor plan network representation.



Fig. 3. Representation of the agent and the variables defined for direction $k$.

where $D_{k,t}$ is the distance from the future position $M_{i,t+1}$ to the projection of the target point on the view range circle [see Fig. 3(a)], $R$ is the depth of the view range and $R_{k,\text{step}}$ is the distance the pedestrian can move in one time step with his free walking speed. In this way, we can obtain the value of $E_k$ with the range of [0, 1].

*2) Interaction Between Pedestrian and Obstacle $O_k$:* This parameter presents the behavior of a pedestrian trying to maintain distance from obstacles. It is represented as a relative value of the distance to the nearest obstacles or the geometry boundaries $D_{k,b}$ [see Fig. 3(b)], i.e.,

$$O_k = \frac{D_{k,b}}{R}. \tag{3}$$

*3) Interaction Between a Pedestrian and Other Pedestrians $P_k$ and $A_k$:* The interactions between one pedestrian and others can be considered in two aspects: 1) people may try to keep distance from each other and, at the same time and 2) avoid potential collision with others in the moving direction. The first aspect can be represented by $P_k$, which is the relative distance from the nearest pedestrian on the direction $k$ [see Fig. 3(b)], i.e.,

$$P_k = \frac{D_{k,p}}{R}. \tag{4}$$

The second aspect can be represented by $A_k$, which is the relative angle $\theta_{k,j}$ between $\vec{v}_k$ and $\vec{v}_j$, where $\vec{j}$ is the movement velocity of the nearest agent within the trajectory of $\vec{v}_k$ [see Fig. 3(c)]. $A_k$ can be calculated by

$$A_k = 1 - \frac{|\theta_{k,i}|}{\pi}. \tag{5}$$

*4) Inertia $I_k$:* This parameter reflects the behavior of a pedestrian that does not change its current movement direction abruptly and frequently. It can be denoted by using the angle between $\vec{v}_k$ and $\vec{v}_c$ and can be calculated as

$$I_k = 1\frac{|\theta_{k,c}|}{\theta/2}. \tag{6}$$

Alternatively, $U_k$ can be also calculated as

$$U_k = E_k = -\frac{\omega_o}{\omega_e'} \cdot (1 - O_k) - \frac{\omega_p}{\omega_e'} \cdot (1 - P_k) - \frac{\omega_a}{\omega_e'}$$
$$\cdot (1 - A_k)\frac{\omega_i}{\omega_e'} \cdot (1 - I_k) + \xi \tag{7}$$

where the weight parameter for $E_k$ is normalized and other weight parameters are represented by the proportion to it. The calculation methods for $U_k$ by using (1) and (7) yield similar simulation results. No significant differences were observed in our simulations, but the approach by (7) may generate more distinguishable utility sets (see Fig. 4 for an example). Equation (7) was used in this paper.

Once a direction $k$ is chosen, an individual can move forward one step according to the available distance and the desired movement speed. That is, $|\vec{v}_k| = \min(v_{a,t}, v_{i,t})$, where $v_{a,t}$ is the movement speed considering the available movement distance, and $v_{i,t}$ is the desired speed of agent $i$ at time $t$. Previous studies tend to control the speed by defining acceleration and deceleration behavior [20], [30], [31], [37]. However, measuring and quantifying the acceleration and deceleration, in reality, pose a real challenge on its application. In fact, previous research on empirical data revealed that speed is definitely related to density [1], [8]. The use of empirical results in
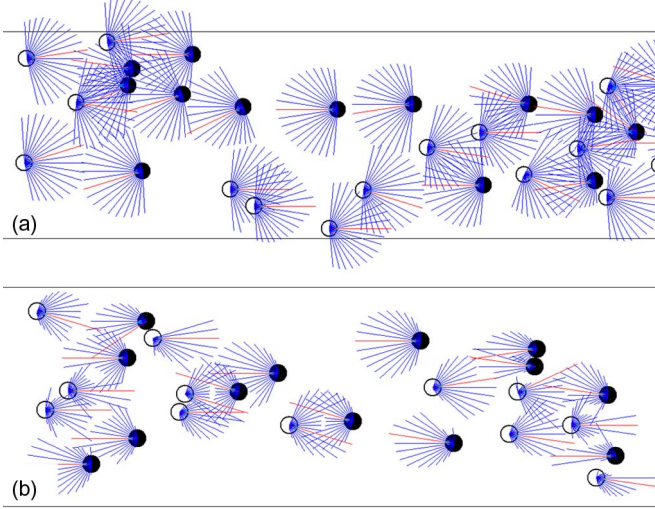
Fig. 4. Samples of relative utility as a proportion to the length of $R/2$. The open and closed circles represent pedestrians moving to the right and the left, respectively; the blue and red lines represent the relative utility; the red lines indicate the direction with the largest utility. (a) Utility sets calculated by (1). (b) Utility sets calculated by (7).

simulation models can control the speed of pedestrians directly and effectively. In this paper, the frequently cited results from Weidmann [14] (as cited in [1]) are used. The desired speed of pedestrians at time $t$ can be obtained as

$$v_{i,t} = v_f \times \left\{ 1 - e^{\left[ -\gamma \left( \frac{1}{\rho_t} - \frac{1}{\rho_{\max}} \right) \right]} \right\} \qquad (8)$$

where $\rho_t$ is the density within the view range at time $t$, $\rho_{\max} = 5.4$ persons/m$^2$ is the maximum density, $\gamma = 1.913$, and $v_f$ is the free walking speed of the pedestrian concerned. The free walking speeds of pedestrians in the model are generated within a reasonable range from the normal distribution of $N(1.34, 0.34^2)$.

## III. PARAMETER SENSITIVITY ANALYSIS

As shown in (7), only $E_k$ provides a positive contribution to $U_k$. All other parameters serve negatively. In this way, evaluating the contribution of every negative parameter for the utility by considering the weight parameters as a proportion of $\omega_e$ will be easier, just as shown in (7). By denoting $\omega_o' = \omega_o/\omega_e'$, we may set $\omega_o' \in [0, 1)$. A value equal to 1 is not preferred to avoid unexpected minus values. The same rule can be applied for other negative parameters. Given that the purpose of the inertia parameter $I_k$ is to maintain the current moving direction and avoid abrupt and frequent changes, the coefficient $\omega_i'$ can be set as small as possible to meet this purpose and, at the same time, not overwhelm the other coefficients. The influences of other coefficients were tested and analyzed as follows.

### A. Interaction With Obstacles

A series of test simulations is carried out to evaluate the sensitivity of the parameter $O_k$ and to adjust its weight parameter $\omega_o'$, where $\omega_o'$ is set to 0.1–0.9 and other negative parameters
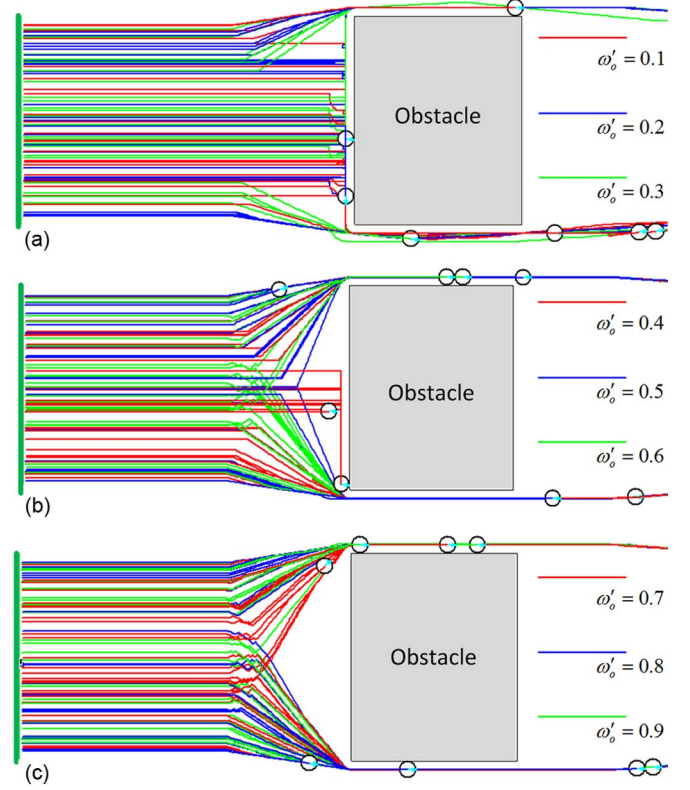


Fig. 5. Comparison of movement trajectories of 80 pedestrians walking over a 5 m × 4 m obstacle with $\omega_o' = 0.1 - 0.9$ and other weight parameters set to zero. (a) $\omega_o' = 0.1$ (red), 0.2 (blue), and 0.3 (green). (b) $\omega_o' = 0.4$ (red), 0.5 (blue), and 0.6 (green). (c) $\omega_o' = 0.7$ (red), 0.8 (blue), and 0.9 (green).

TABLE I
PERCENTAGE OF PEDESTRIANS WHO CHANGED MOVEMENT DIRECTION $P$ IN THE SIMULATION TEST FOR PARAMETER $\omega_o'$

| $\omega_o'$ | 0.1 | 0.2 | 0.3 | 0.4 | 0.5 | 0.6 | 0.7 | 0.8 | 0.9 |
|---|---|---|---|---|---|---|---|---|---|
| P (%) | 11.2 | 27.4 | 35.3 | 76.5 | 100 | 100 | 100 | 100 | 100 |

are set to zero to minimize the disturbance. The setup of the simulation is shown in Fig. 5.

Eighty pedestrians walk from the green line at the left, around the rectangular obstacle, and reach the target behind the obstacle. The trajectory of each pedestrian is recorded by different colors according to the value of $\omega_o'$ for that pedestrian. Table I shows the percentages of pedestrians who changed movement directions to avoid the obstacle in advance. It is shown that the larger the value of $\omega_o'$, the more likely the pedestrian will try to navigate around the obstacle (see Fig. 5 and Table I). The value between 0.4 and 0.6 may serve as a critical value for this transition to the obstacle-avoiding behavior. Considering the effect of other parameters, $\omega_o' = 0.4$ is used in the rest of the simulations.

### B. Interaction With Other Pedestrians

As discussed in Section II, the interactions with other pedestrians can be represented from the point of interperson distance $P_k$ and the movement direction discrepancy $A_k$. For pedestrians moving at opposite directions, the two parameters
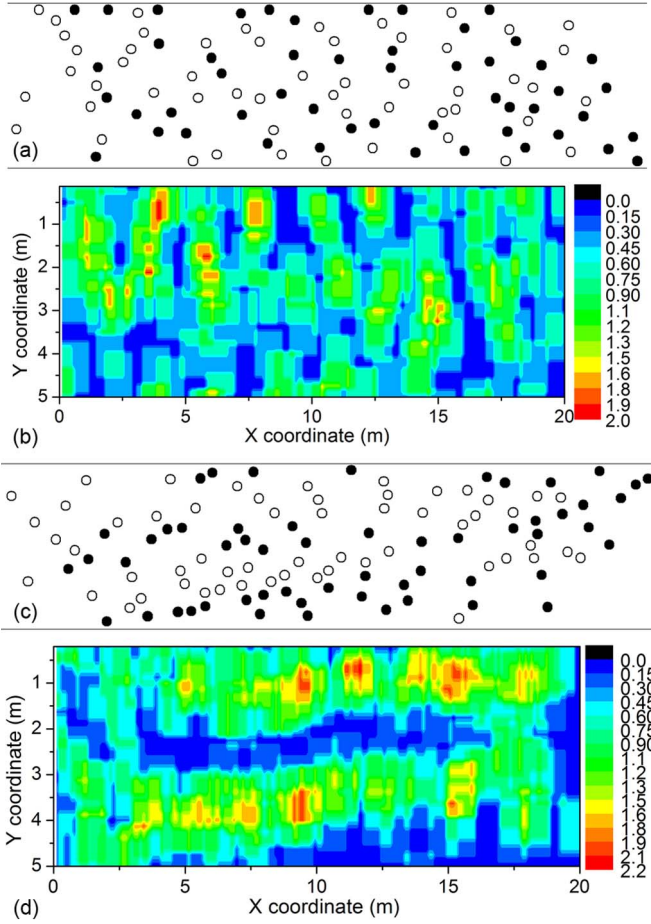
Fig. 6. Simulation snapshots and right walkers' density distributions of the bidirectional pedestrian flow in a 20 m × 5 m corridor with different hybrid interperson coefficient settings. (a) Snapshot for simulation with $\omega_{p,a} = 6$: open circles represent pedestrians walking to the right, and closed circles represent pedestrians walking to the left. (b) Density distribution of right walkers in correspondence with (a): the density is calculated for every 1-m² area for an average of 10 s. (c) Snapshot for simulation with $\omega_{p,a} = 1$. (d) Density distribution of right walkers in correspondence with (c).

try to separate two pedestrians to avoid possible collision. However, for pedestrians moving at the same direction, $P_k$ still provides a separation force between two pedestrians, whereas $A_k$ tries to "adhere" pedestrians with similar directions. That is, they compete with each other under this situation. In order to evaluate their contribution to the overall utility, we define this as a "hybrid interperson coefficient," which is denoted by the relative value of $\omega_p'$ to $\omega_a'$: $\omega_{p,a} = \omega_p'/\omega_a'$. $\omega_{p,a}$ represents the relative strength of $P_k$ to $A_k$.

A test simulation is also performed for this purpose. In this test simulation, pedestrians walk from the right and left open boundaries through the 20 m × 5 m corridor to the opposite side (see Fig. 6). The density distributions of pedestrians walking to the right (open circles in Fig. 6) are plotted when $\omega_{p,a} = 6$ [see Fig. 6(a) and (b)] and $\omega_{p,a} = 1$ [see Fig. 6(c) and (d)]. It can be seen that when $\omega_{p,a} = 6$, the pedestrians moving at the same direction are dispersed from each other, whereas when $\omega_{p,a} = 1$, they tend to move following the pedestrians ahead, and a dynamic lane of pedestrians appears. Based on the simulation animations, a stronger tendency of following behavior and clearer lanes of pedestrians with a smaller value
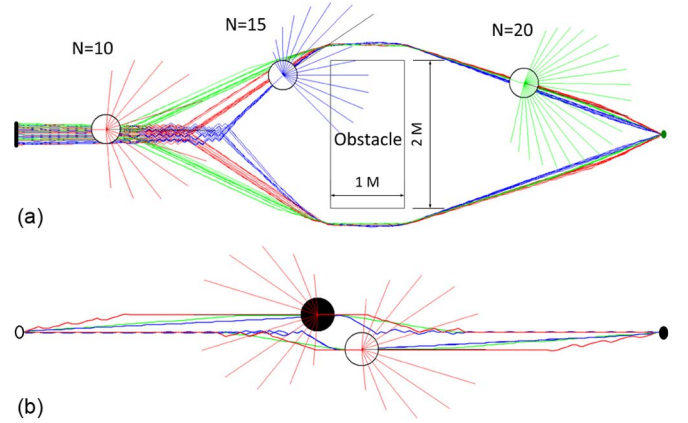


Fig. 7. Performance of different view angle discretization resolutions shown as the trajectories of (a) 80 pedestrians steering around an obstacle or (b) 60 pedestrians moving oppositely in pairs. Different values of $N$ are represented in different colors: $N = 10$ (red), $N = 15$ (blue), and $N = 20$ (green). Lines on a circle represent relative utilities as the proportion to the length of $R/2$. Right moving preference is used in (b) but not in (a). The weight parameters are set as $\omega_o' = 0.4$ and others are zero in (a), whereas $\omega_p' = 0.6$, $\omega_a' = 0.3$, and others are zero in (b).

of $\omega_{p,a}$ within the range of 1–6 occur. However, values smaller than 1 are not considered in this study because of the unrealistic pedestrian queue pattern.

### C. Effect of View Angle Discretization Resolution

As introduced above, the view angle $\theta$ of an agent is discretized into uniformly distributed $N$ subangles $\Delta\theta = \theta/N$. Thus, $N$ represents the resolution of the view angle discretization. Aside from the computational burden that significantly increases with increasing $N$, the most significant effect of different values of $N$ on the simulation results lies in the steering behavior around obstacles or other agents. The performances of selected discretization resolutions, including $N = 10$, 15, and 20, are shown in Fig. 7.

The reacting distance varies for different values of $N$. A larger value of $N$ may result in higher mobility of the agent and leads to earlier reacting to obstacles or other agents and smoother trajectories. For example, the trajectories when $N = 20$ in Fig. 7 are smoother than when $N = 10$. However, an odd number $N$ can produce an unsymmetrical distribution of subangles in the left and right sides of the agent, which will lead to even more unstable steering behaviors and abrupt changes of direction (such as the situation shown in Fig. 7 when $N = 15$). Despite the different performances of different view angle discretization resolutions, it should be noted that the steering behavior in real pedestrian traffic is complex and many other more important factors may be involved. Thus, selecting $N$ in the model is generally involved to balance computational efficiency and accuracy. Moreover, an odd number should be avoided.

### IV. MODELING OF PEDESTRIAN BEHAVIOR

Based on the aforementioned understanding of these parameters and coefficients, we also conducted simulations for examining the model's ability on modeling some basic pedestrian flow
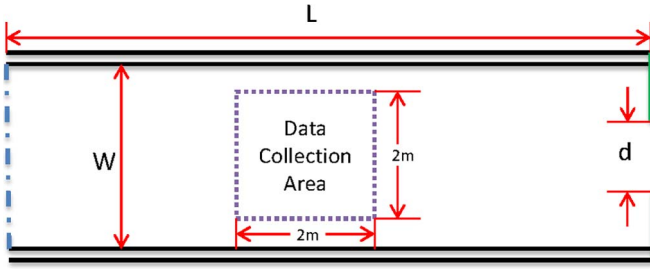
Fig. 8. Illustration of the corridor setup for simulation. The corridor has a width $W = 3$ m, length $L = 15$ m, open boundaries at the left and the right, and the width of the right boundary $d$ is changeable.

dynamics. Typically, there are three kinds of pedestrian flow scenarios that are usually considered the most basic pedestrian movement phenomena and referred to as the benchmarks for most of the pedestrian flow studies, including the unidirectional flow [2], [4] [14], the bidirectional flow [21], [22], and the flow through a bottleneck [3], [5], [9]–[11]. Field observations and laboratory studies have been carried out to understand the relationships between system dimensions and pedestrian behavior, such as the so-called fundamental diagrams and the flow rates through bottlenecks [1].

Here, the model developed in this paper is used to simulate the pedestrian flow through a corridor (see Fig. 8). The results are compared with published empirical data, part of which was downloaded from the website http://www.ped-net.org. The width of the corridor is $W = 3$ m and the length is $L = 15$ m. The right side of the corridor is designed as a door with flexible width, which can be changed according to simulation needs. Different scenarios can be achieved by adjusting the flow rates at the left and right open boundaries and the width of the door at the right boundary. The weight parameters in (7) are set as $\omega'_o = 0.4$, $\omega'_p = 0.6$, $\omega'_a = 0.3$, and $\omega'_i = 0.1$.

### A. Density and Velocity Relationship

As mentioned before, previous studies tried to produce a fundamental diagram to present the basic relationships between density and speed or flow rate. The simplest pedestrian flow phenomenon should be the unidirectional flow through a corridor. In this paper, the unidirectional pedestrian flow through the corridor shown in Fig. 8 is studied. In the simulation, the pedestrians walk from the left boundary to the right boundary. Different density conditions are achieved by dynamically adjusting the flow rate from the left boundary and the width $d$. In general, different density and velocity calculation methods can be used for pedestrian flow [12]. These methods are basically consistent with one another. In this paper, an area of 2 m × 2 m is selected to extract the flow data (see Fig. 8). The density and average of the instantaneous movement velocity of all the pedestrians within this area are recorded every 5 s.

The results are plotted and compared with published empirical data sets in Fig. 9. Weidmann's [14] data set is a review work through combining and formulating the results from many other different studies. The results of Môri and Tsukaguchi [4] and Hankin and Wright [2] are obtained by observing the pedestrian flow in sidewalks or the passages in subway stations,
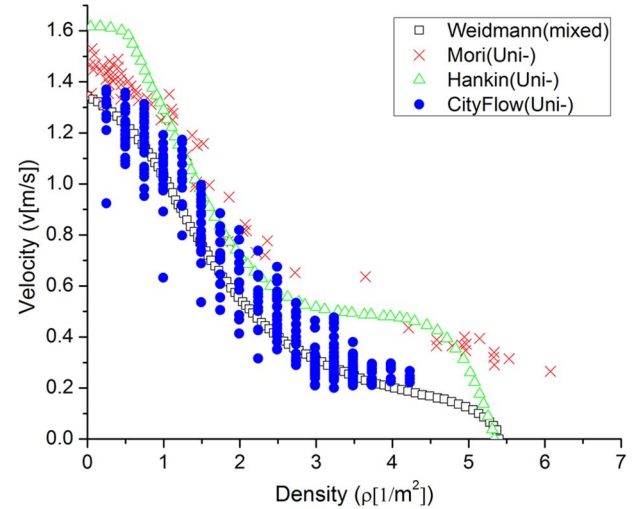


Fig. 9. Relationship between density and movement velocity in modeling the unidirectional pedestrian flow in a corridor and the comparison with published empirical results.

which should be able to represent pedestrian behavior under normal conditions. The overall distribution of the data points is basically consistent with these observation results. However, fluctuations in velocity can be found at the same density levels. Setting the initial free walking speeds as normal distribution and the data collection method used here may be the reasons for this result. Densities higher than 4.5 persons/m² can be only observed in front of the bottleneck in our simulation and are not shown in this diagram.

### B. Flow Rate at Bottlenecks

Flow rates in persons per second or the specific flow rate in persons per second per meter at the positions of bottlenecks are one of the most important parameters for planning and designing facilities, such as a door or a passageway. Various published field survey results on flow rate were collected from different scenarios. Most of these results suggest that flow rate is nearly in a linear relationship with the width of the bottleneck. A recent study has also pointed out that it should not be regarded as a linear relationship if other factors are considered [7]. In this paper, the pedestrian flow from the left boundary of the corridor in Fig. 8 through the door with changeable width at the right boundary is studied. The width of the door $d$ is tested with different values from 0.8 to 2.0 m, and the flow rate at the left boundary is set to full capacity to guarantee that the maximum flow rate can be reached at the door. The flow rates at the door under different door widths are plotted in Fig. 10. It is shown that the flow rates can achieve maximum values and remain steady after around 180 s. The flow rate gradually increases with increasing door width. Maximum flow rates under different door widths are also compared with field observation results (see Fig. 11). Five different research results are cited here for this purpose, including the laboratory observation data collected by Müller et al. [3] (as cited in [1]), Muir et al. [5], Nagai et al. [9], Kretz et al. [10], and Seyfried et al. [11]. The flow rates are consistent with Müller's results when the door width is less than 1.2 m. However, the specific flow slightly
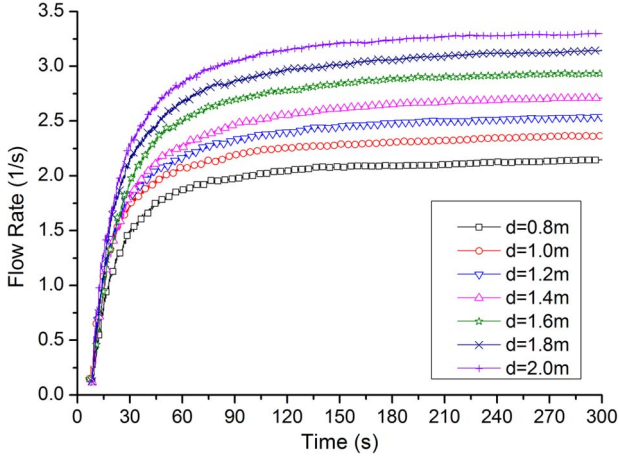
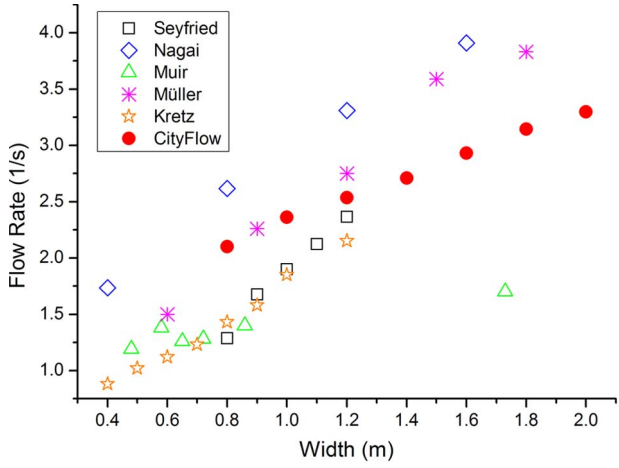Fig. 10. Plot of flow rate against time at the door with different widths $d = 0.8-2.0$ m in the simulation.



Fig. 11. Maximum flow rate at the door under different widths and comparison with empirical data.
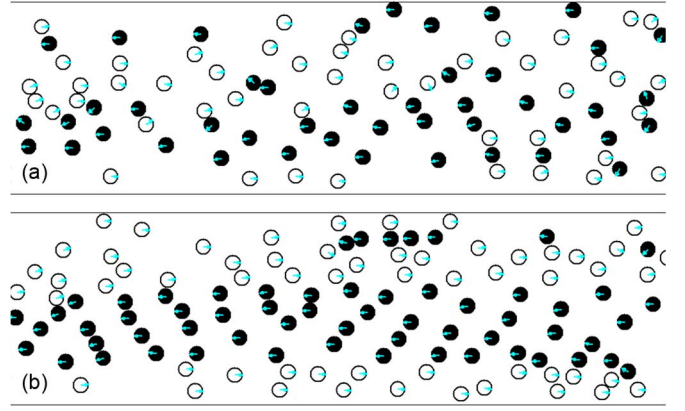


Fig. 12. Simulation snapshots of the lane formation phenomenon in bidirectional pedestrian flows; open circles and closed circles represent the pedestrians moving to the right and to the left, respectively. (a) Bidirectional flow under medium density (20% system capacity). (b) Bidirectional flow under high density (40% system capacity).
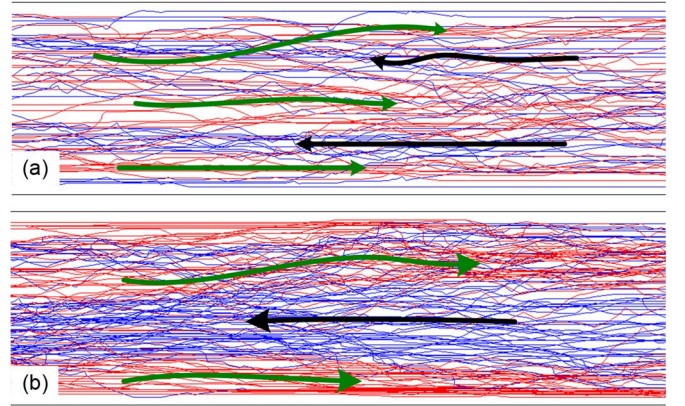


Fig. 13. Trajectories of the pedestrians moving to the right (red lines) and to the left (blue lines) in the simulation of the bidirectional pedestrian flow. (a) Bidirectional flow under medium density (20% system capacity). (b) Bidirectional flow under high density (40% system capacity).

decreases when the door width is wider than 1.2 m. This result may be due to the slight limitation of the corridor dimension on the crowding effect at the door area. Door width below 0.8 m is not shown in this diagram since there would be a small probability (about 5%) that a deadlock status will occur around the door area.

### C. Lane Formation in the Bidirectional Flow

As a complex system, pedestrian crowd movement may perform various self-organization phenomena. The formation of pedestrian walking lanes in the bidirectional pedestrian flow is one of the most important phenomena studied by researchers [21], [22]. As mentioned in Section III-B, the interpersonal movement direction parameter $A_k$ tries to "adhere" pedestrians with similar directions. When the hybrid interperson coefficient $\omega_{p,a} = 1$, pedestrians in the same direction tend to move following the pedestrians ahead. In this way, the model introduced in this paper can produce the lane-formation phenomenon in bidirectional pedestrian flow scenarios.

Fig. 12 shows the simulation snapshots for the bidirectional pedestrian flow in a corridor with 5 m width under two density levels. Fig. 13 shows the collection of movement trajectories of these pedestrians in simulations corresponding to Fig. 12. Pedestrian walking lanes can be observed explicitly in simulations under both the medium-density level and the high-density level. However, under the medium-density level, more lanes are shown in a dynamic manner, and the agents change lanes more frequently. Meanwhile, the lanes under the high-density level are steadier and may include more pedestrians for each lane.

### V. SUMMARY

This paper has presented a pedestrian flow simulation tool, namely, CityFlow, by focusing on the introduction of the agent-based microscopic pedestrian flow simulation model used in CityFlow. CityFlow is implemented through two modules: the route choice and map navigation module and the agent-based individual movement module. The agent-based pedestrian flow simulation model treats every pedestrian as an agent in the shape of a circle with a view range. Agents move one step

per time step toward the direction calculated by a utility maximization approach in which various factors that influence pedestrian's movement are considered.

The sensitivities of the parameters in the agent-based model were analyzed by running a series of simulation experiments. For the parameter $O_k$, which represents interactions with obstacles, the larger the value of the coefficient $\omega_o'$, the more likely the pedestrian will try to navigate around the obstacle. Values between 0.4 and 0.6 may serve as a critical value for the transition of this obstacle-avoiding behavior between different statuses. The interpersonal distance parameter $P_k$ and the movement direction discrepancy parameter $A_k$ compete with each other when the movement direction of the pedestrian to be decided is the same as the one detected. The proportion of their coefficients $\omega_{p,a}$ can be used to denote the relative strength of these two factors. The discussion on the performances of different view angle discretization resolutions revealed that the selection of $N$ in the model involves balancing the computational efficiency and accuracy. However, an odd number should be avoided.

The model was also validated by modeling several basic pedestrian flow phenomena and comparing the simulation results with published empirical data. First, the unidirectional pedestrian flow through a corridor was simulated. The density and speed relationships in the simulation were plotted and compared with the pedestrian flow fundamental diagrams produced from previous field or laboratory studies. The distribution of density–speed data sets was basically consistent with the empirical results obtained for densities below 4.5 persons/m$^2$. Second, the model performance at bottlenecks was investigated by simulating pedestrians walking through a door with the changeable width from 0.8 to 2.0 m. The curve of the flow rates against simulation time and the maximum flow rates at the door with different widths were presented. The simulation results were comparable with the empirical observation results derived from observations in subway stations, particularly for the door width less than 1.2 m. Finally, the model's ability to model the bidirectional pedestrian flow was also investigated. Results show that the model could reproduce the lane-formation phenomenon. Moreover, the simulation results revealed that the pedestrian flow lanes were more dynamic in the medium-density condition than in the high-density condition.

The model can be used for studying pedestrian traffic problems such as the passenger flow in a metro station or other scenarios with similar system sizes. However, as a microscopic model based on continuous space, its computing efficiency may be apparently lower than that of grid-based discrete models. For larger size of areas with more agents, the computational complexity would increase significantly and become unacceptable. This limitation may be weakened naturally with the ever fast-growing computing technology. Moreover, this paper has focused on the modeling of operational level microscopic pedestrian movement behaviors, but not the strategic and tactical level route choice and planning behaviors. For practical applications, an extension of the model for more sophisticated strategic and tactical level behaviors would be necessary, which will be one of our future works.

## REFERENCES

[1] A. Schadschneider, D. Chowdhury, and K. Nishinari, "Pedestrian dynamics," in *Stochastic Transport in Complex Systems*. Amsterdam, The Netherlands: Elsevier, 2011, pp. 407–460.

[2] B. D. Hankin and R. A. Wright, "Passenger flow in subways," *Oper. Res.*, vol. 9, no. 2, pp. 81–88, Jun. 1958.

[3] K. Müller, "Zur gestaltung und bemessung von fluchtwegen für die evakuierung von personen aus bauwerken auf der grundlage von modellversuchen," Ph.D. dissertation, Tech. Hochschule, Otto von Guericke Univ. Magdeburg, Magdeburg, Germany, 1981.

[4] M. Môri and H. Tsukaguchi, "A new method for evaluation of level of service in pedestrian facilities," *Transp. Res. A, Gen.*, vol. 21, no. 3, pp. 223–234, May 1987.

[5] H. C. Muir, D. M. Bottomley, and C. Marrison, "Effects of motivation and cabin configuration on emergency aircraft evacuation behavior and rates of egress," *Int. J. Aviation Psychol.*, vol. 6, no. 1, pp. 57–77, Jan. 1996.

[6] W. Daamen and S. P. Hoogendoorn, "Free speed distributions—Based on empirical data in different traffic conditions," in *Proc. Pedestrian Evac. Dyn. 2005*, N. Waldau, P. Gattermann, H. Knoflacher, and M. Schreckenberg, Eds., 2007, pp. 13–25.

[7] S. M. V. Gwynne, E. D. Kuligowski, J. Kratchman, and J. A. Milke, "Questioning the linear relationship between doorway width and achievable flow rate," *Fire Safety J.*, vol. 44, no. 1, pp. 80–87, Jan. 2009.

[8] A. Seyfried, B. Steffen, W. Klingsch, and M. Boltes, "The fundamental diagram of pedestrian movement revisited," *J. Stat. Mech., Theory Exp.*, vol. 2005, no. 10, p. P10002, Oct. 2005.

[9] R. Nagai, M. Fukamachi, and T. Nagatani, "Evacuation of crawlers and walkers from corridor through an exit," *Phys. A, Stat. Mech. Appl.*, vol. 367, pp. 449–460, Jul. 2006.

[10] T. Kretz, A. Grunebohm, and M. Schreckenberg, "Experimental study of pedestrian flow through a bottleneck," *J. Stat. Mech., Theory Exp.*, vol. 2006, no. 10, p. P10014, Oct. 2006.

[11] A. Seyfried, O. Passon, B. Steffen, M. Boltes, T. Rupprecht, and W. Klingsch, "New insights into pedestrian flow through bottlenecks," *Transp. Sci.*, vol. 43, no. 3, pp. 395–406, Aug. 2009.

[12] J. Zhang, W. Klingsch, A. Schadschneider, and A. Seyfried, "Transitions in pedestrian fundamental diagrams of straight corridors and T-junctions," *J. Stat. Mech., Theory Exp.*, vol. 2011, no. 6, p. P06004, Jun. 2011.

[13] B. Steffen and A. Seyfried, "Methods for measuring pedestrian density, flow, speed and direction with minimal scatter," *Phys. A, Stat. Mech. Appl.*, vol. 389, no. 9, pp. 1902–1910, May 2010.

[14] U. Weidmann, "Transporttechnik der fussgänger," in *Transporttechnische Eigenschaften des Fussgängerverkehrs,* 2nd ed. Zurich, Switzerland: ETH Zürich, Mar. 1993, ser. Schriftenreihe des IVT Nr. 90.

[15] R. L. Hughes, "A continuum theory for the flow of pedestrians," *Transp. Res. B, Methodol.*, vol. 36, no. 6, pp. 507–535, Jul. 2002.

[16] A. Shende, M. P. Singh, and P. Kachroo, "Optimization-based feedback control for pedestrian evacuation from an exit corridor," *IEEE Trans. Intell. Transp. Syst.*, vol. 12, no. 4, pp. 1167–1176, Dec. 2011.

[17] N. Pelechano and A. Malkawi, "Evacuation simulation models: Challenges in modeling high rise building evacuation with cellular automata approaches," *Autom. Constructr.*, vol. 17, no. 4, pp. 377–385, May 2008.

[18] M. Chraibi, U. Kemloh, A. Schadschneider, and A. Seyfried, "Force-based models of pedestrian dynamics," *Netw. Heterogeneous Media*, vol. 6, no. 3, pp. 425–442, Sep. 2011.

[19] C. Burstedde, K. Klauck, A. Schadschneider, and J. Zittartz, "Simulation of pedestrian dynamics using a two-dimensional cellular automaton," *Phys. A, Stat. Mech. Appl.*, vol. 295, no. 3/4, pp. 507–525, Jun. 2001.

[20] D. Helbing and P. Molnar, "Social force model for pedestrian dynamics," *Phys. Rev. E, Stat. Nonlin. Soft Matter Phys.*, vol. 51, no. 5, pp. 4282–4286, May 1995.

[21] Y. Tajima, K. Takimoto, and T. Nagatani, "Pattern formation and jamming transition in pedestrian counter flow," *Phys. A, Stat. Mech. Appl.*, vol. 313, no. 3/4, pp. 709–723, Oct. 2002.

[22] J. Ma, W. G. Song, J. Zhang, S. M. Lo, and G. X. Liao, "$k$-nearest-neighbor interaction induced self-organized pedestrian counter flow," *Phys. A, Stat. Mech. Appl.*, vol. 389, no. 10, pp. 2101–2117, May 2010.

[23] S. Xu and H. B. L. Duh, "A simulation of bonding effects and their impacts on pedestrian dynamics," *IEEE Trans. Intell. Transp. Syst.*, vol. 11, no. 1, pp. 153–161, Mar. 2010.

[24] J. Dai, X. Li, and L. Liu, "Simulation of pedestrian counter flow through bottlenecks by using an agent-based model," *Phys. A, Stat. Mech. Appl.*, vol. 392, no. 9, pp. 2202–2211, May 2013.

[25] R. Y. Guo, S. C. Wong, H. J. Huang, P. Zhang, and W. H. K. Lam, "A microscopic pedestrian-simulation model and its application to

intersecting flows," *Phys. A, Stat. Mech. Appl.*, vol. 389, no. 3, pp. 515–526, Feb. 2010.

[26] T. Saegusa, T. Mashiko, and T. Nagatani, "Flow overshooting in crossing flow of lattice gas," *Phys. A, Stat. Mech. Appl.*, vol. 387, no. 16-17, pp. 4119–4132, Jul. 2008.

[27] S. B. Liu, L. Z. Yang, T. Y. Fang, and J. Li, "Evacuation from a classroom considering the occupant density around exits," *Phys. A, Stat. Mech. Appl.*, vol. 388, no. 9, pp. 1921–1928, May 2009.

[28] N. Chooramun, P. J. Lawrence, and E. R. Galea, "An agent based evacuation model utilising hybrid space discretisation," *Safety Sci.*, vol. 50, no. 8, pp. 1685–1694, Oct. 2012.

[29] S. M. Lo, Z. Fang, P. Lin, and G. S. Zhi, "An evacuation model: The SGEM package," *Fire Safety J.*, vol. 39, no. 3, pp. 169–190, Apr. 2004.

[30] M. Asano, T. Iryo, and M. Kuwahara, "Microscopic pedestrian simulation model combined with a tactical model for route choice behaviour," *Transp. Res. C, Emerging Technol.*, vol. 18, no. 6, pp. 842–855, Dec. 2010.

[31] G. Antonini, M. Bierlaire, and M. Weber, "Discrete choice models of pedestrian walking behavior," *Transp. Res. B, Methodol.*, vol. 40, no. 8, pp. 667–687, Sep. 2006.

[32] N. Pelechano, J. M. Allbeck, and N. I. Badler, "Controlling individual agents in high-density crowd simulation," in *Proc. ACM SIGGRAPH/ Eurograph. Symp. Comput. Animation*, San Diego, CA, USA, 2007, pp. 99–108.

[33] D. Helbing, "Agent-based modeling," in *Social Self-Organization*, D. Helbing, Ed. Berlin, Germany: Springer-Verlag, 2012, pp. 25–70.

[34] S. Bandini, S. Manzoni, and G. Vizzari, "Agent based modeling and simulation," in *Encyclopedia of Complexity and Systems Science*, R. A. Meyers, Ed. New York, NY, USA: Springer-Verlag, 2009, pp. 184–197.

[35] S. Bandini, S. Manzoni, and G. Vizzari, "Situated cellular agents: A model to simulate crowding dynamics," *IEICE Trans. Inf. Syst.*, vol. E87-D, no. 3, pp. 669–676, Mar. 2004.

[36] S. P. Hoogendoorn, "Pedestrian flow modeling by adaptive control," *Transp. Res. Rec., J. Transp. Res. Board*, vol. 1878, pp. 95–103, 2004.

[37] M. Moussaid, D. Helbing, and G. Theraulaz, "How simple rules determine pedestrian movement and crowd disasters," *Proc. Nat. Acad. Sci. USA*, vol. 108, no. 17, pp. 6884–6888, Apr. 2011.

[38] S. P. Hoogendoorn and P. H. L. Bovy, "Pedestrian route-choice and activity scheduling theory and models," *Transp. Res. B, Methodol.*, vol. 38, no. 2, pp. 169–190, Feb. 2004.

**Siuming Lo** received the Ph.D. degree in architecture from the University of Hong Kong, Pokfulam, Hong Kong.

He is a Professor with the Department of Civil and Architectural Engineering, City University of Hong Kong, Kowloon, Hong Kong. He has received many research grants by the Hong Kong Research Grant Council in studying building and large-scale evacuation, fire risk modeling, system dynamics modeling, crowd movement, etc. He has extensively published in various international refereed journals and conferences. His research interests include building and urban design, spatial planning for pedestrian flow and evacuation, decision support system, and fire safety engineering.
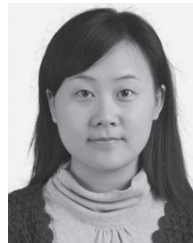
**Jian Ma** received the B.E. degree in safety engineering from University of Science and Technology of China, Hefei, China, in 2005 and the Ph.D. degree in safety technology and engineering from City University of Hong Kong, Kowloon, Hong Kong, in 2010.

From 2011 to 2012, he further performed studies on pedestrian traffic and evacuation dynamics as a Postdoctoral Fellow with City University of Hong Kong. He is currently an Associate Professor with the National United Engineering Laboratory of Integrated and Intelligent Transportation, School of Transportation and Logistics, Southwest Jiaotong University, Chengdu, China. His research interests include pedestrian traffic, crowd dynamics, emergency evacuation, and intelligent traffic simulation.

Dr. Ma is a reviewer for international journals such as IEEE TRANSACTIONS ON INTELLIGENT TRANSPORTATION SYSTEMS.

**Shaobo Liu** received the B.E. degree from Xi'an University of Architecture and Technology, Xi'an, China, in 2007, the M.E. degree from University of Science and Technology of China, Hefei, China, in 2010, and the Ph.D. degree from City University of Hong Kong, Kowloon, Hong Kong, in 2013.

He is now a Postdoctoral Fellow with the Centre for Systems Informatics Engineering, City University of Hong Kong. His research interests include pedestrian and evacuation dynamics, crowd behaviors under normal and emergency situations, and transportation planning.

**Weili Wang** received the B.E. and M.E. degrees in the geographical information system from Wuhan University, Wuhan, China, in 2009 and 2011, respectively. She is currently working toward the Ph.D. degree in pedestrian engineering at City University of Hong Kong, Kowloon, Hong Kong.

Her research interest includes the pedestrian flow simulation and behavior analysis, evacuation planning based on Geographical Information System, data mining and analysis for passenger mobility pattern, and the interaction with built environment.